Effect of Applied Voltage on Diameter and Morphology of Ultrafine Fibers in Bubble Electrospinning

Yong Liu,[1,2] Liang Dong,[1,2] Jie Fan,[1,2] Rui Wang,[1,2] Jian-Yong Yu[3]

[1]*Tianjin and Ministry of Education Key Laboratory of Advanced Textile Composite Materials, Tianjin Polytechnic University, Tianjin, People's Republic of China*
[2]*School of Textiles, Tianjin Polytechnic University, Tianjin, People's Republic of China*
[3]*Modern Textile Institute, Donghua University, Shanghai, People's Republic of China*

Received 17 December 2009; accepted 14 August 2010
DOI 10.1002/app.33203
Published online 19 October 2010 in Wiley Online Library (wileyonlinelibrary.com).

ABSTRACT: A novel electrospinning process, bubble electrospinning, was used to produce porous nonwoven fibrous mats, of which the fiber diameter can range from nano- to microscales. The deformation of a charged bubble, from which multiple jets were ejected, was observed using a high-speed motion camera. The effects of different applied voltages on diameter, morphology, and structure of bubble-electrospun ultrafine fibers were theoretically analyzed and then experimentally validated by scanning electron microscopy and atomic force microscopy. The results showed that the average diameter of fibers increased with the increase of the applied voltage in bubble electrospinning, which is quite different from that in traditional electrospinning process under the similar conditions. The number of beaded fibers decreased with increasing applied voltage. Additionally, the crystallinities of polyvinylpyrrolidone ultrafine fibers obtained in this process were higher than that of polyvinylpyrrolidone powders. The production rate of bubble electrospinning was higher than that of the traditional electrospinning. © 2010 Wiley Periodicals, Inc. J Appl Polym Sci 120: 592–598, 2011

Key words: bubble electrospinning; ultrafine fibers; applied voltage; morphology; mass production

INTRODUCTION

Electrospinning has become an attractive technique for the fabrication of polymer fibers, with diameters ranging from the submicron scale down to a few nanometers, and it has generated significant interest because of its potential impact in many applications such as biomedicine,[1,2] textiles,[3] filters,[4] and others.[5] These applications require large number of electrospun fibers. However, the major challenges encountered in the electrospinning process are poor efficiency and low output, which become the bottleneck that affects its development. To increase the production rate of ultrafine and nano fibers, many new electrospinning processes were invented. The simplest way is to use multiple nozzles in a single electrospinning procedure, which can be arranged together into various patterns such as a line,[6–8] a circle,[7] or a matrix.[6,9,10] The major flaw in this approach is mutual electric interaction of multiple charged jets, which might result in instability of the spinning procedure.[6] Yarin and Zussman[11] proposed a two-layer system, with the lower layer being a ferromagnetic suspension and the upper layer a polymer solution, to produce multiple jets in an electric field. David et al.[12] showed a cleft electrospinner in which the needle was replaced by two metallic plates and a cleft between them. Some researchers[13,14] described electrospinning of polymer ultrafine and nano fibers from multiple jets on a porous tubular surface. Up to now, it is said that a roller electrospinning under the name of Nanospider[TM,15] which is based on a rotating cylinder solution-feeding system,[16] is the only successful commercialization of electrospinning for mass production of ultrafine and nano fibers. Recently, our group[17–20] invented and patented a new electrospinning method, bubble electrospinning, for large-scale ultrafine and nano fiber production. The mechanism of this process is deceptively simple and primarily based on the produced bubbles on the liquid surface. Each bubble in this process is similar to a Taylor cone in traditional electrospinning process. However, previous studies focused on the principle of this process and fabrication of nanofibers. Ren and He[21] studied the effect of concentration on the spinning procedure. Yang et al.[22] reported the relationship between the minimal fiber diameter and the applied voltage in bubble electrospinning. However, the average fiber diameter is

Correspondence to: Y. Liu (liuyong@tjpu.edu.cn).

Contract grant sponsor: Key Project of Chinese Ministry of Education; contract grant number: 210006.
Contract grant sponsor: National Science Foundation of Tianjin; contract grant number: 10JCYBJC02200.
Contract grant sponsor: Tianjin Universities Science and Technology Development Fund; contract grant number: 20080322.
Contract grant sponsor: National Natural Science Foundation of China; contract grant numbers: 51003073 (Liu), 10972053 (He), 10802021 (Xu), and 10872048 (Yu).

Journal of Applied Polymer Science, Vol. 120, 592–598 (2011)

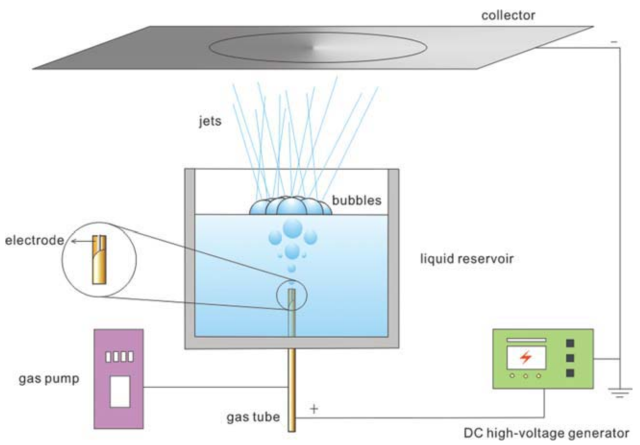

Figure 1 Schematic drawing of bubble electrospinning process. [Color figure can be viewed in the online issue, which is available at wileyonlinelibrary.com.]

generally regarded as having a significant influence on the properties of electrospun fiber mat. To understand this process, a common water-soluble polymer, polyvinylpyrrolidone (PVP) was used to produce fiber mat in bubble electrospinning process in this study. The deformation of bubble and multiple jets were observed by a high-speed camera, and morphologies of fiber mats obtained at various applied voltages in bubble electrospinning were examined by scanning electron microscopy and atomic force microscopy (AFM), respectively.

EXPERIMENTAL

Experimental setup

Shown in Figure 1 is the experimental setup of bubble electrospinning process, which consists of a vertical solution reservoir (a glass cup Φ80 mm) having a top opening, a gas tube installing at the bottom center of the reservoir, a metal thin electrode fixed along the centerline of the tube, a gas pump, an DC high-voltage generator (0-100 KV, F180-L, Shanghai Fudan High School, Shanghai, China), and a grounded flat metal plate as collector over the reservoir. The tube and the electrode were inserted through the bottom of the reservoir and connected with the gas pump and the generator, respectively. The polymer solution is placed inside the reservoir. One or several bubbles will be produced on the free surface of the polymer solution when the gas pump is turned on slowly. The shape of bubble will be changed from spherical to conical as an DC electric field is applied. When the applied voltage exceeds the threshold voltage, multiple jets were observed ejecting from the bubbles to the collector.

Materials

Two polymers PVP (k-30, $\overline{M}_w = 30{,}000–40{,}000$ g/mol) and polyethylene oxide (PEO, $\overline{M}_w = 500{,}000$ g/mol) were purchased from Sinopharm Chemical Reagent Co., Ltd., (Shanghai, China) and Shanghai Lian Sheng Chemical Co., Ltd., (Shanghai, China), respectively. The solvents, pure alcohol, and the distilled water were obtained from Shanghai Chemical Co., Ltd., (Shanghai, China). All the chemicals were used as received without further purification. The polymer was dissolved into a solvent mixture of pure alcohol/distilled water with the weight ratio of 9 : 1. The PVP solution concentration was adjusted to 36 wt %, and the PEO concentration was adjusted to 2%. All the mixtures were stirred with mechanical stirrer for 2 hr at room temperature.

Characterization

The morphology, surface microstructure, and crystallinity of the PVP fiber mat obtained by bubble electrospinning process was investigated by a scanning electron microscope (JSM-5610; JEOL, Japan), an atomic force microscope (AFM.IPC-208B; Chongqing University, Chongqing, China), and X-ray diffraction (XRD) analysis (Rigaku D/max 2550 PC; Rigaku Co., Tokyo, Japan), respectively. A high-speed motion camera, Redlake's MotionXtra system (HG-LE; Redlake Inc., USA), and an digital compact camera (FE-160; Olympus, Japan) were used to capture the motion of jets and other phenomena in the experiment.

RESULTS AND DISCUSSION

Deformation of a charged bubble

Taylor cone was described by G. I. Taylor[23] in 1964 and is a requirement in the electrospinning and electrospraying processes. When the applied voltage reaches the threshold value, a bubble in the electric field will become instable and breaking. Vanhille and Campos-Pozuelo[24,25] have recently proved theoretically that a broken bubble had many special properties that could be used for fiber fabrication. In bubble electrospinning process, the compressed gas is released inside the solution, which will produce one or several bubbles on the free surface of the solution. When the bubble is exposed to an electric field, the shape of bubble deforms from spherical to conical. Figure 2 is the real-time photos of a bubble in this process recorded by a high-speed motion camera at 1000 frames per second. Initially, the bubble is spherical [Fig. 2(a)]; when a voltage is applied, the bubble is stretched upward and deformed to oval shape [Fig. 2(b)], and finally to a conical shape [Fig. 2(c)], and the whole process takes about 17 msec. From the conical bubble, a jet is ejected, and then the bubble bursts and further splits into numerous jets. Almost the whole liquid film is broken into thin jets. Then, the next bubble was produced, and the process was repeated until

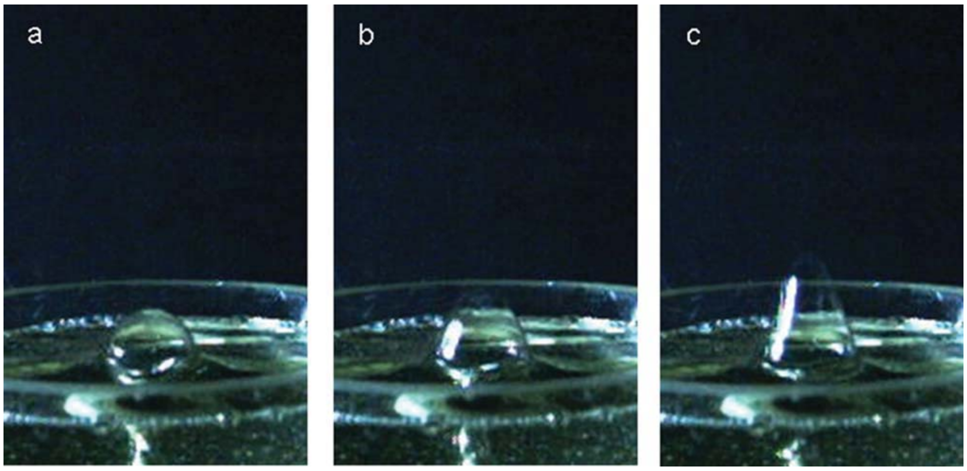

Figure 2 Deformation of a bubble under electric force (a) 0 msec, (b) 8 msec, and (c) 17 msec. [Color figure can be viewed in the online issue, which is available at wileyonlinelibrary.com.]

the polymer solution was used up. Figure 3 shows the real-time photo of a stable bubble and multiple jets in bubble electrospinning, which was recorded by a digital compact camera.

Effect of applied voltage on morphology and diameter of ultrafine fibers

It is well known that in traditional electrospinning process the applied voltage is one of the most important parameters that can influence the formation of ultrafine and nano fibers, so does in bubble electrospinning process.

The velocity of jet in electrospinning process can be expressed as

$$u = u_0 + at \tag{1}$$

where u is the velocity of jet, u_0 is the initial velocity of the jet, a is the acceleration of the jet, and t is the acceleration time.

According to Newton's second law,

$$F = ma \tag{2}$$

where m is the mass of jet and a is the acceleration.

According to Coulomb's law,

$$F = qE \tag{3}$$

where F is the electric force, q is the unit positive charge, and E is the electric field strength.

To simplify calculations, here we assume the electric field is a uniform electric field in bubble electrospinning process. Thus,

$$F \propto E \propto U \tag{4}$$

where U is the applied voltage.

Generally, the jet obtained in the electrospinning process is usually cylindrical in shape. The Navier-Stokes equation for each viscous columned jet of this process[26] is

$$\rho\pi r^2 dz \frac{Du}{Dt} = g\pi r^2 \rho dz + 2\pi r\sigma E dz + \pi r^2 \frac{d\tau}{dz} dz \tag{5}$$

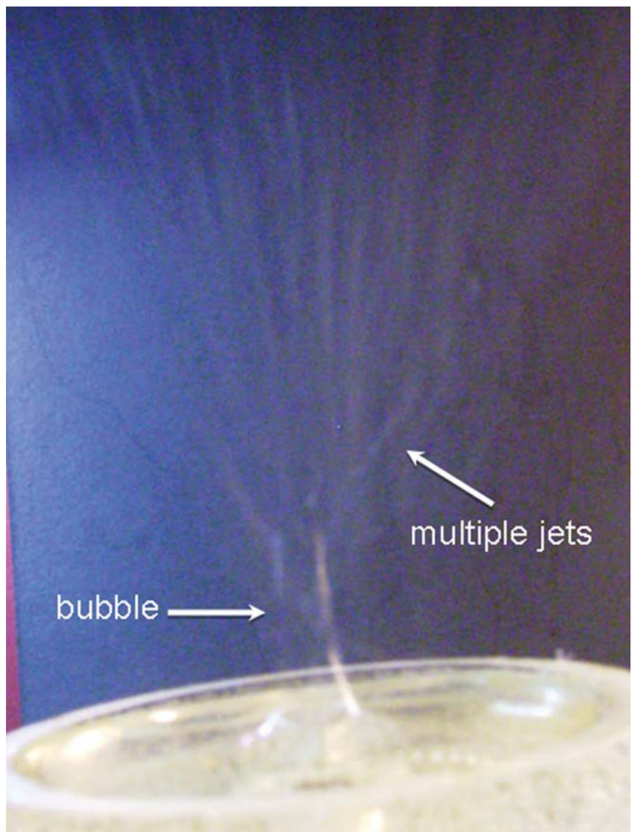

Figure 3 Multiple jets in bubble electrospinning process. [Color figure can be viewed in the online issue, which is available at wileyonlinelibrary.com.]

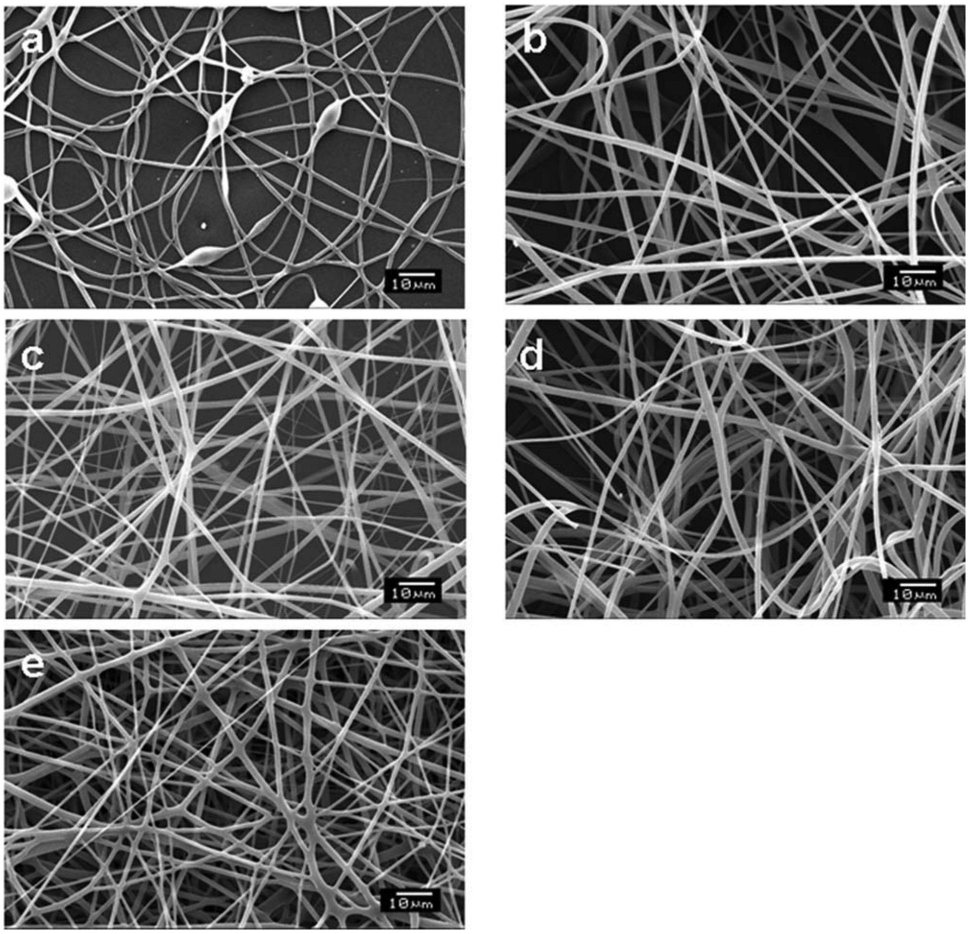

Figure 4 Scanning electron microscopy micrographs (a–e) of bubble-electrospun fibers at applied voltages (16, 20, 25, 30, and 35 kV). All the bars are 10 μm.

where ρ is the density of jet, *r* is the radius of the fiber, σ is the surface charge density of the jet fluid, which is assumed to remain unchanged during the electrospinning, τ the viscous resistance, *g* the gravitational acceleration, *dz* is the length of an unit volume in the direction of the flow, and *u* and *r* are, respectively, the velocity and diameter of the jet.

The applied voltage is the main force pulling the bubble into jets in bubble electrospinning, and all the other forces can be neglected.[22] Additionally, the density of jet can be considered constant because of the unit volume. We can get

$$\frac{Du}{Dt} = a \propto \frac{2\sigma E}{r} \propto \frac{2\sigma U}{r} \tag{6}$$

Under the above assumption that a spatially uniform electric field is applied, the acceleration, *a*, can be considered constant. We predict

$$r \propto U \tag{7}$$

Our analysis reveals that the fiber diameter will be increased with the increase in the applied voltage in bubble electrospinning process.

To evaluate the above analysis, experiments were performed with different applied voltages. In these experiments, the effect of the applied voltage on the morphology and the average fiber diameter were

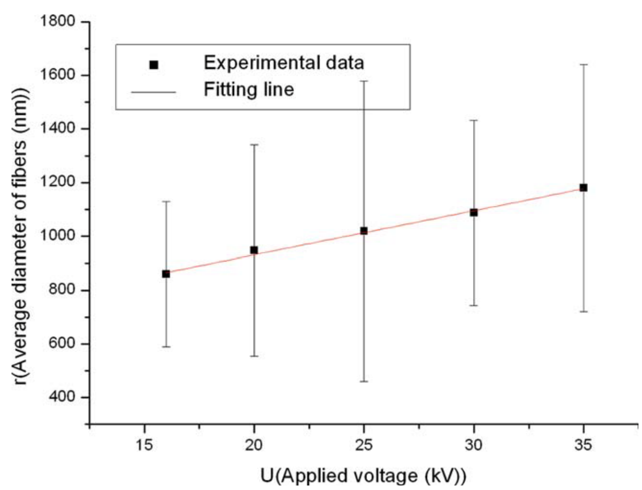

Figure 5 Effect of the applied voltage on the average fiber diameter. [Color figure can be viewed in the online issue, which is available at wileyonlinelibrary.com.]

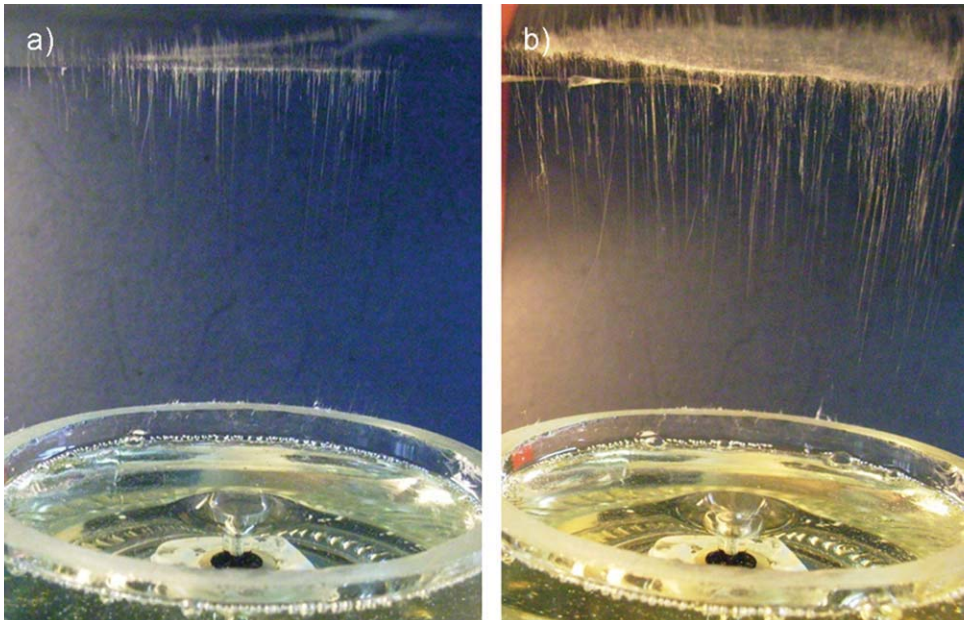

Figure 6 Multiple jets at different applied voltages, 20 and 35 kV, respectively. [Color figure can be viewed in the online issue, which is available at wileyonlinelibrary.com.]

studied in the range of 16–35 kV, whereas all other processing parameters were kept constant (spinning distance = 8 cm, gas pressure = 3 kPa, solution concentration = 36 wt %, and time = 120 sec). Figure 4 shows scanning electron microscopy micrographs of morphologies of bubble electrospun PVP fibers from 36 wt % solutions of PVP in a mixture of pure alcohol/distilled water (9 : 1, w/w) at applied voltages of 16, 20, 25, 30, and 35 kV, respectively. The results show that the fiber diameters range from tens of nanometers to several micrometers, which is similar to that in traditional electrospinning process. The average diameter of fibers increases from 860 to 1180 nm, with the increase in the applied voltage from 16 to 35 kV in the experiments (Fig. 5). Equation (6) is the fitting equation of the experimental data, which shows that the experimental data agree well with the theoretical analysis.

$$r = 16U + 612.7 \tag{8}$$

Additionally, the reason for the increase in the average diameter of fibers might be that a higher applied voltage leads to a higher electrostatic force, which causes more jets (Fig. 6), even those larger-diameter jets which may be unavailable at the low electrostatic force. Figure 6 presents the real-time photos of bubble electrospinning processes at applied voltages of 20 and 35 kV, respectively. As can be seen in Figure 6, the number of jets at high applied voltage was obviously more than that at low applied voltage. Meanwhile, those thin jets, which can be available at the low applied voltage, will be stretched strongly enough to produce thinner fibers when the applied voltage is increased. Figure 7 illustrates the values of the minimum diameter of nanofibers at the different applied voltages, corresponding to Figure 4(a–e), respectively. The experimental data are in agreement with those reported by Yang et al.[22]

Additionally, some beads appeared in fiber mat when the applied voltage was low [Fig. 4(a)], which may be the reason that the bead cannot be drawn into cylindrical fiber at lower electric force, similar to that in traditional electrospinning process.[27]

The XRD patterns of PVP fibers obtained at different applied voltages, 25, 30, and 35 kV, respectively, are given in Figure 8. The XRD pattern of PVP fibers showed peaks that were intense and sharp,

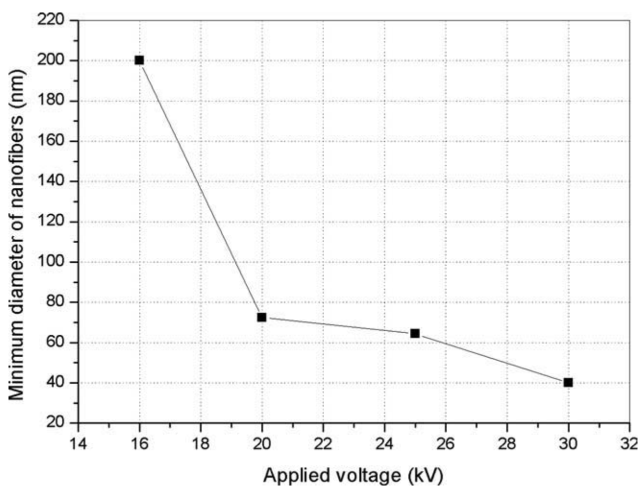

Figure 7 Effect of the applied voltage on the minimal fiber diameter.

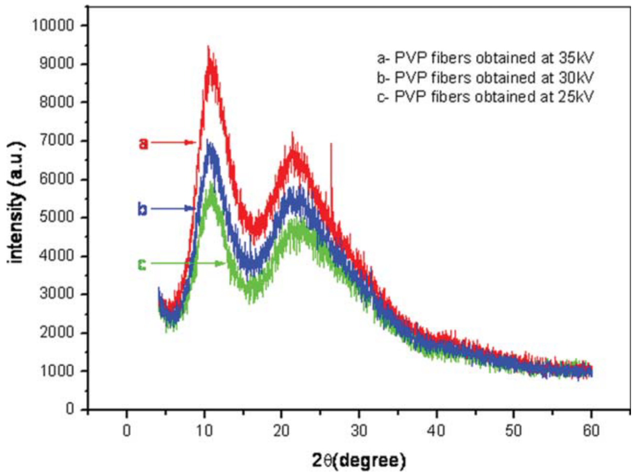

Figure 8 XRD patterns of PVP fibers obtained at different applied voltages. [Color figure can be viewed in the online issue, which is available at wileyonlinelibrary.com.]

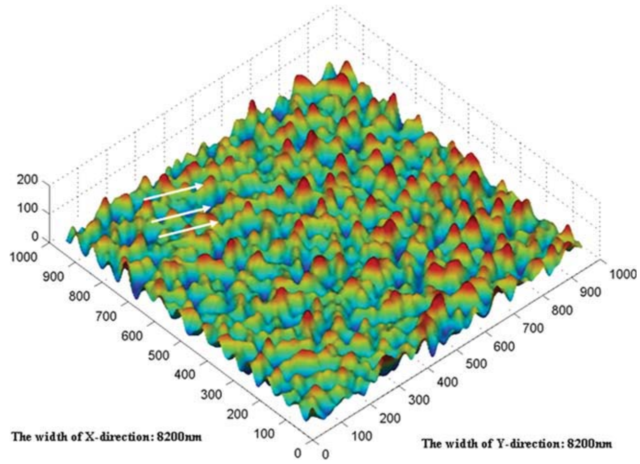

Figure 9 AFM surface topography image of bubble-electrospun fiber mat. [Color figure can be viewed in the online issue, which is available at wileyonlinelibrary.com.]

indicating its crystalline nature. The two broad peaks around $2\theta = 11.7^0$ and $2\theta = 21.14^0$ are the characteristic peaks of PVP polymer. The crystallinities of fibers obtained at 25, 30, and 35 kV are 40% ± 2.97%, 41.96% ± 2.56%, and 42.48% ± 4.61%, respectively. Considering the possible calculation error of the crystallinity, it shows that there is no much difference among these fibers obtained at different applied voltage in this process. However, compared with the crystallinity, 34.11% ± 2.71%,[5] of original PVP powder, each value of the above crystallinities of fibers is greater than that of PVP powder, which shows that the crystallinity of PVP is significantly affected by the bubble electrospinning process.

Morphology of ultrafine fiber mat

To study the morphology and surface microstructure of the fiber mat in this process, an atomic force microscope was used to observe the topography of the mat surface. Shown in Figure 9 is the AFM surface topography image at the 8.2 × 8.2 μm scale of bubble-electrospun fiber specimen. In the AFM image, the "ridges" are the fibers (arrows in Fig. 9), the red "peaks" are the fibers curving over and intercrossing irregularly with one another, and the blue "valleys" are the porosities among the fibers, respectively. These results demonstrate that the fibrous mat produced by bubble electrospinning has characteristic features such as rough surface and high porosity, which are beneficial in many applications, e.g., superhydrophobic fabric.

Production rate and potential

To study the production rate of fibers produced by bubble electrospinning, we measured the weight of the obtained fiber mat. In the traditional electrospinning, the weight of the fiber mat obtained from a single needle is typically 0.1–1.0 g/hr.[16] To measure the production rate of fibers, the obtained mat was produced with a single bubble after 120 sec of bubble electrospinning and then weighed. The output of fibers per hour was calculated by multiplying the above weight by 30. The experimental result shows that the yield of ultrafine and nano fibers can reach 7.5 g/hr using a single bubble electrospinning. It shows that the production rate in this electrospinning is higher than that in traditional

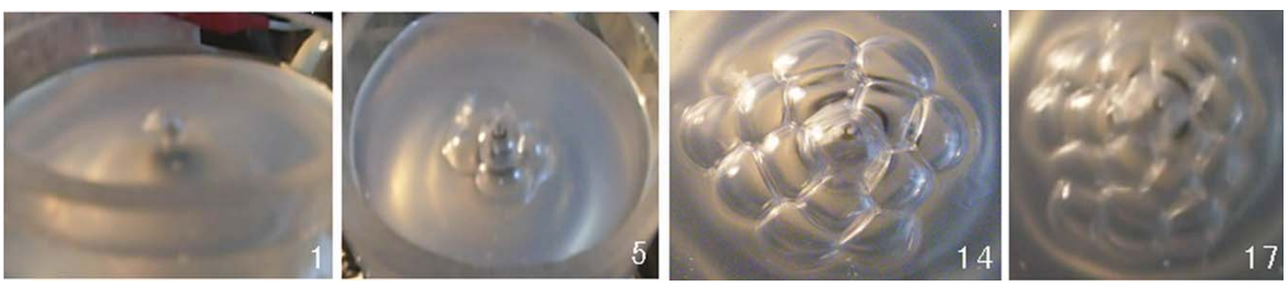

Figure 10 Photos of different number of bubbles produced by a single gas tube in PEO solution. [Color figure can be viewed in the online issue, which is available at wileyonlinelibrary.com.]

electrospinning. In addition, we tried to produce several or even scores of bubbles on the surface of polymer solution to greatly increase its output in the future. A 2 wt % PEO solution was used in the experiment. Adjusting to the gas pressure, there was different number of bubbles produced on the surface of PEO solution at appropriate conditions, as shown in Figure 10. The number of bubbles on liquid surface was 1, 5, 14, and 17. The result shows that the bubble electrospinning method has great potential for mass production of ultrafine and nano fibers.

CONCLUSIONS

We successfully developed bubble electrospinning as a new candidate for producing polymer fibers with high efficiency. By releasing the compressed gas in the PVP or PEO solution, one or several bubbles were observed on the solution surface. In bubble electrospinning process, multiple jets were ejected from the bursting bubble. The average diameter of fibers increased with the increase in the applied voltage, whereas the minimal diameter of the obtained fibers deceases with the increase in the applied voltage. The experimental results showed that the fiber mat in this process has characteristic features such as rough surface and high porosity, and the production rate of bubble electrospinning was much higher.

References

1. Agarwal, S.; Wendorff, J. H.; Greiner, A. Polymer 2008, 49, 5603.
2. Prabhakaran, M. P.; Venugopal, J.; Chyan, T. T.; Hai, L. B.; Chan, C. K.; Tang, A. L. Y.; Ramakrishna, S. Tissue Eng A 2008, 14, 1.
3. Schreuder-Gibson, H.; Gibson, P.; Senecal, K.; Sennett, M.; Walker, J.; Yeomans, W.; Ziegler, D.; Tsai, P. P. J Adv Mater 2002, 34, 44.
4. Yoon, K.; Hsiao, B. S.; Chu, B. J Membr Sci 2009, 338, 145.
5. He, J.-H.; Liu, Y.; Mo, L.-F.; Wan, Y.-Q.; Xu, L. Electrospun Nanofibres and Their Applications; Smithers Rapra Technology: Shropshire, UK, 2008.
6. Theron, S. A.; Yarin, A. L.; Zussman, E.; Kroll, E. Polymer 2005, 46, 2889.
7. Tomaszewski, W.; Szadkowski, M. Fibres Textile East Eur 2005, 13, 22.
8. Ding, B.; Kimura, E.; Sato, T.; Fujita, S.; Shiratori, S. Polymer 2004, 45, 1895.
9. Kim, G. H.; Cho, Y.-S.; Kim, W. D. Eur Polym J 2006, 42, 2031.
10. Varesano, A.; Carletto, R. A.; Mazzuchetti, G. J Mater Process Tech 2009, 209, 5178.
11. Yarin, A. L.; Zussman, E. Polymer 2004, 45, 2977.
12. David, L.; Arindam, S.; Pavel, P. J Appl Phys 2008, 103, 084309.
13. Dosunmu, O. O.; Chase, G. G.; Kataphinan, W.; Reneker, D. H. Nanotechnology 2006, 17, 1123.
14. Varabhas, J. S.; Chase, G. G.; Reneker, D. H. Polymer 2008, 49, 4226.
15. Cengiz, F.; Jirsak, O. Fiber Polym 2009, 10, 177.
16. Zhou, F.-L.; Gong, R.-H.; Porat, I. Polym Int 2009, 58, 331.
17. Liu, Y.; He, J.-H. Int J Nonlinear Sci Numer Simul 2007, 8, 393.
18. Liu, Y.; He, J.-H.; Xu, L.; Yu, J.-Y. J Polym Eng 2008, 28, 55.
19. He, J.-H.; Liu, Y.; Xu, L.; Yu, J.-Y.; Sun, G. Chaos Soliton Fract 2008, 37, 643.
20. Dong, L.; Liu, Y.; Fan, J.; Kang, W.-M.; Wang, R.; Cheng, B.-W.; Xu, L. Nonlinear Sci Lett D 2010, 1, 129.
21. Ren, Z.-F.; He, J.-H. J Appl Polym Sci, to appear.
22. Yang, R.; He, J.; Xu, L.; Yu, J. Polymer 2009, 50, 5846.
23. Taylor, G. I. Proc Roy Soc Lond Ser A 1964, 280, 383.
24. Vanhille, C.; Campos-Pozuelo, C. Int J Nonlinear Sci Numer Simul 2008, 9, 367.
25. Vanhille, C.; Campos-Pozuelo, C. Int J Nonlinear Sci Numer Simul 2009, 10, 751.
26. Liu, Y.; Dong, L.; Fan, J.; Kang, W.-M.; Wang, R.; Xu, L.; Cheng, B.-W.; Yu, J.-Y. Nonlinear Sci Lett A 2010, 1, 239.
27. Liu, Y.; He, J.-H.; Yu, J.-Y.; Zeng, H.-M. Polym Int 2008, 57, 632.